

24 the difference was observed in the boundary for two-individual group. The intermittencies for the inter-
25 distances of two individuals in the boundary and the central areas were markedly different before and
26 after treatment. When the differences between the intermittencies in the boundary and the central areas
27 and between “before” and “after” treatment are considered, the distribution patterns of the shadowing
28 time (scaling behaviors or intermittency patterns) should be a useful means of bio-monitoring to detect
29 contaminants in the environment.

30

31 PACS numbers: 02.50.Ey, 02.50.Fz, 45. 70.Cc

32 Keywords: Intermittency, Shadowing time, Movement, Chemical stress, Force, Collective motion,
33 Boundary

34

35 *Email: tschon@pusan.ac.kr;

36 Fax: +82-51-512-2262

37

38 I. INTRODUCTION

39 The analysis of the response behaviors of animals has received considerable attention regarding *in*
40 *situ* monitoring of indicator species since computational methods and interfacing techniques were
41 introduced in the 1980's [1-4]. Monitoring by using behavioral changes is ecologically relevant,
42 economical and faster than monitoring by using method of chemical detection [5-7]. Due to the high
43 degree of complexity in behavioral data, however, various computational methods have been proposed
44 to exploring time-series data on animal movements [1, 8]: parameterization with a fractal dimension [9]
45 and permutation entropy [10, 11], statistical methods using correlation analyses [10, 12, 13], data
46 transform including Fourier transforms [7, 14] and wavelet analysis [15]. Considering the complexity
47 of behavioral data, informatics has been further applied to movement patterns, including self-

48 organizing map [7, 14, 16] and multi-layer perception [6, 15], and is capable of identifying specific
49 response behaviors of indicator species under chemical stress. Because of the uncertainties in
50 behavioral patterns, the hidden Markov model has been used to analyze behavioral state changes after
51 exposure to chemical treatment [16, 17]. However, the abovementioned reports mostly focused on data
52 for single individuals, and not many studies were conducted on the responses of multiple individuals.

53 Regarding group formation by multiple individuals, simulation models based on the equations of
54 motion have been proposed to elucidate the collective behavior associated with self-propelled particle
55 systems according to the group (i.e., overall average orientation) and the neighbor (e.g., attraction,
56 repulsion) responses [18-23]. Group behavior models were also analyzed, and observed data were
57 evaluated; force components of individuals in collective motion were calculated in order to explain the
58 relationship between the individual itself, its neighbors and environmental factors [24, 25]; individual
59 fish movements were expressed by using the mass, drag coefficient, and external forces. Recently, the
60 importance of nearest-neighbor interactions in group formation was addressed [26, 27].

61 In this study, we focused on the physical forces produced by one and two individuals under stressful
62 conditions due to chemical exposure. In order to reveal the structure property in the movement data, we
63 addressed the probability distributions of the shadowing time in time-series force data on fish observed
64 in a confined area. Scaling behavior has been increasingly used in analyzing movement behavioral
65 patterns of animals in the wild and in the laboratory. Intermittency is defined as the probability
66 distribution of the shadowing time during which the data are consecutively higher than a threshold
67 number [28-31]. For time-series data generated from a chaotic system (e.g., attractor), intermittency
68 exhibits a universal algebraic scaling at high frequencies with a slope approximately $-3/2$ while it
69 exhibits an exponential scaling at lower frequencies [28, 30].

70 Intermittency is among the universal mechanisms that produce chaos from a periodic orbit in
71 a continuous way [32] and has been reported in various fields, including coordination of muscular

72 systems [33, 34], chemical kinetics [35, 36], laser models [37], and fluid dynamics [38]. In ecology,
73 flow intermittency regarding biodiversity determination in stream ecosystems has been recently
74 investigated [39, 40]. Intermittency has been further applied to behavior studies. Harnos *et al.* [41]
75 analyzed scaling and intermittency in the temporal behavior of nesting gilts, reporting that the time
76 spent by a gilt in a given form of activity had a power-law probability distribution, and showed the
77 intermittent occurrence of certain periodic behavioral sequences to indicate a critical state. Mashnova *et*
78 *al.* [42] investigated intermittency and a truncated power law in aphid movement and addressed the
79 alternate appearance of fast and slow movement phases that were distinguished by a threshold value of
80 velocity. However, intermittency in response behavior of animals under chemical stress has not been
81 extensively studied.

82 In addition to chemical response, we further observed individual movement at different locations in a
83 confined area. Although test animals can move around in a more-or-less straightforward manner over a
84 wide range, the individuals are constrained inside a confined arena within a boundary, especially for
85 behavior monitoring within an observation arena [16]. The boundary zone was considered to be the
86 area in which free movement would be minimally allowed, and is important for the life events,
87 including protection and exploitation, of animals [43, 44]. We showed that the scaling behaviors of
88 two individuals of *D. rerio* would be different at the boundary and the central areas of the observation
89 arena before and after chemical treatment. Specifically, we intended to characterize intermittency in
90 response behaviors in three different categories, 1) comparison of one and two individuals, 2) boundary
91 and central areas, and 3) before and after chemical treatment. We analyzed the probability distributions
92 of the shadowing time to address changes in the structure property in the movement data and found that
93 intermittency in individual and group movement could be used as a possible means of behavioral
94 monitoring.

95

II. EXPERIMENTS

1. Test Organisms

One and two individuals of zebrafish, *D. rerio*, were observed under chemical stress. Due to vulnerability to chemical stress and availability of biological information (e.g., genomics, physiological responses), the zebrafish is considered to be one of the most suitable vertebrate model organisms for various biological tests [45-47], including behavior assessment [7, 16, 48]. The species has a strong potential for being an indicator in risk assessment [16, 49]. Individuals of wild-type *D. rerio* were obtained from a local fish dealer for stock population (300 individuals) and were reared for 2 weeks before observation [50] at a temperature of $25 \pm 1^\circ\text{C}$ and pH of 7.1 ± 0.3 under a light/dark cycle of 14/10 h, light on at 7:00 h and off at 20:00 h [51]. Two fluorescent lights (26 J/s) were placed 50 cm above the rearing container. Tap water was filtered with air stones under air compression (DT - 10F, Chuang Xing Electric Appliances[®]) after dechlorination for three days. Fishes were fed dry food (Nutron Hi - Fi, PRODAC[®]) twice a day (once a day on weekends). Other rearing conditions are described below [16].

Test organisms (ages: 5 – 6 months; body lengths: 30 – 40 mm) were randomly chosen from the stock population and were placed individually in a glass aquarium (300 mm × 300 mm × 300 mm; water height of 20 mm). Before observation, organisms were acclimated to the observation system for 30 minutes [50]. To simplify observation and minimize noise, food and oxygen were not supplied to the arena during the observation period. Two 13J/s fluorescent lights were provided 50 cm above the water's surface and the two light sources were symmetrically 32 cm away from the center over the observation arena. Other rearing and observation conditions were the same as those used to rear the stock population.

Formaldehyde (HCHO, 37wt. % solution in water, A.C.S. reagent, Gamma-Aldrich[®]) was used as a source of stress to the test organisms. Formaldehyde is claimed to be one of most toxic environmental

120 hormones and a possible carcinogenic agent through bioaccumulation [52]. The chemical was directly
121 added to the water in the observation aquarium at a concentration of 1 ppm. In order to minimize noise,
122 the chemical was delivered through an injector (Pipetman® P20) connected to the observation
123 aquarium through a flexible polyethylene tube (1.85 mm in diameter and 1 m in length) after dilution
124 with a proper amount of water.

125 **2. Observations and Recording**

126 The observation system consisted of an observation aquarium, a camera (Logitech®Vid™HD), a PC
127 (Intel® Core™ 2 Duo CPU E4500@ 2.20GHz), and software for tracking the motion of multiple
128 individuals. The software was developed in the Ecosystem and Behavior Lab. at Pusan National
129 University based on stereo vision [53] after evaluation with a multiple individual tracking program
130 (SynthEyes, 2008, Anderson Technologies LLC). The x - y position of each individual was continuously
131 recorded at 30 frames per second from a top view in two dimensions before (30 minutes) and after (30
132 minutes) treatment. Five-minute segments were selected for analysis according to Suzuki *et al.* [27] and
133 Herbert-Read *et al.* [54]. After treatment, fish immediately responded to olfactory stimulus from the
134 chemical for approximately 5 minutes, showing abnormal behaviors including shaking and turning.
135 Afterwards abnormal behaviors occurred less frequently. Movement tracks for the initial five minutes
136 were analyzed before and after treatment.

137 Based on preliminary research [16, 55], a time segment of 0.2 s for recording movement was selected
138 for this study. Because we aimed to observe overall movement changes of the fish specimens in two
139 dimensions in response to the chemical treatment, the 0.2 s segment was sufficiently short for
140 presenting the displacement of organism location [7, 14]. Extremely short-time response behaviors due
141 to intoxication (e.g., compulsion, trembling) may be expressed in timer shorter than 0.2 s, but this type
142 of behaviors of extremely short duration was not analyzed in this study [16]. Each movement segment
143 was determined with three points with two consecutive 0.1 s segment (0.2 s in total). The observation

144 was repeated 20 times for each group of one and two individuals. Mean values of the linear and the
145 angular speeds were obtained from movement segments for each individual during the observation
146 period; subsequently, the mean values were calculated from the averages of all individuals (i.e., $n = 20$,
147 and 40 for the one- and the two-individual groups, respectively) before and after treatment.

148 **3. Computational Methods**

149 3.1. Determination of boundary and central areas

150 Although test animals can move in a more-or-less straightforward manner (i.e., free run length), the
151 individuals are also located inside a confined arena for monitoring the observation arena, as stated
152 above [16]. We defined the boundary and the central areas by measuring the velocity of single
153 individuals. Figures 1(a) and (b) show the distributions of the x - and the y -component of the velocity
154 along each coordinate before treatment, respectively. In order to determine the boundary area, we
155 inspected the cumulative sum of the velocity data. In Figures 1(c) and (d), the cumulative sums of the
156 two components of the velocity from the sides of the arena are presented.

157 Subsequently, the cumulative sum were fitted with the exponential function $A(1 - e^{-\alpha x})$, here A is a
158 proper amplitude and α is the damping parameter, which is taken as the inverse of the width of
159 boundary. By fitting the data with the exponential function, the boundary width in x -coordinates was
160 evaluated as 19.23 mm and 10.53 mm at the left and the right sides of the x -coordinate and 20.00 mm
161 and 10.53 mm at the left and the right sides of the y -coordinate. From the evaluated value of the width
162 of boundary area from the edge of each side, the largest value, 20.00 mm, was chosen to define the
163 boundary area. The obtained value was comparable to the boundary areas empirically based on the fish
164 size [16].

165 3.2. Real forces of each individual

166 Based on our empirical data, we measured changes in the forces on the test individuals before and
 167 after treatment. Following the framework of classical mechanics, we defined the total force \vec{f}_i on the
 168 i^{th} focal fish as the sum of two real forces, the frictional force \vec{f}_i^{fric} and self-driven force \vec{f}_i^d :

$$169 \quad \vec{f}_i = \vec{f}_i^d + \vec{f}_i^{\text{fric}}, \quad (1)$$

170 with

$$171 \quad \vec{f}_i = m\vec{a}_i \quad (2)$$

$$172 \quad \vec{f}_i^{\text{fric}} = \mu\vec{v}_i, \quad (3)$$

173 where m is the mass of the fish, and μ is the friction coefficient in water. However, in our analysis, the
 174 mass m is set to unity, and μ is assumed to be 0.05 [21].

175 To calculate the self-driven force \vec{f}_i^d , we calculated the velocity and the acceleration of i^{th} individual
 176 at time t by using $\vec{v}_i = \frac{\Delta\vec{r}_i}{\Delta t}$, $\vec{a}_i = \frac{\Delta\vec{v}_i}{\Delta t}$ from the movement tracks. We directly calculated the x - and the
 177 y -components and the absolute force for the one-individual group while forces were calculated
 178 according to center of mass, individual forces, and the relative coordinate between two individuals in
 179 the two-individual group.

180 3.3. Calculation of intermittency

181 The mean value of the absolute of the force measured before treatment was used as a criterion to
 182 determine the threshold for the shadowing time (Figure 2). We used one fourth of the mean value as the
 183 threshold, after testing various levels of the threshold from one eighth to 2 times the mean value. One
 184 fourth the mean value was most suitable in characterizing the probability distributions of the shadowing
 185 time in the boundary and the central areas, as well as “before” and “after” treatment. The threshold
 186 value based on the absolute value of force was also used for the x -component and the y -component.

187 The shadowing times and their probability distributions were expressed on a logarithmic scale. The
188 slopes and the elevations were obtained using a regression analysis [56]. The probability distribution of
189 shadowing times of long duration was also fitted to an exponential curve when breakpoints occurred in
190 intermittency [28, 30].

191 III. RESULTS

192 Figure 3 shows the probability distributions of the shadowing time for forces on individuals observed
193 in the boundary and the central areas when the time duration was selected according to the threshold
194 (95.51 mm/s^2) in one- and two-individual groups. For the x - and the y -components of the forces, the
195 probability distributions of the shadowing time were overall similar between the boundary and the
196 central areas, but were different between one- and two-individual groups (Figures 3(a) – (b), (d) – (e),
197 (g) – (h), and (j) – (k)). Linearity across different shadowing times was observed for the one-individual
198 group (Figures 3(a) – (f)) whereas the linearity was not sustained and probability patterns appeared in
199 the curve for the two-individual group (Figures 3(g) – (l)). The slopes of the distribution became
200 steeper for long-time duration (i.e., right-hand side of the x -axis) for the short-time duration. For the x -
201 and the y -components, the probability distributions of the shadowing time in the boundary area
202 (Figures 3(a) – (b)) appeared to be slightly steeper than that in the central area (Figures 3(d) and (e)),
203 but no statistical difference was observed in the regression lines according to their slopes ($p > 0.05$) [56].

204 For the absolute forces, although the probability distributions of shadowing time were, in general,
205 similar to the x - and the y -components, a difference was observed to some degree in the shapes of the
206 probability distributions (Figures 3(c), (f), (i), and (l)). Before treatment in the boundary area, for
207 instance, the log abundance for the long-time duration appeared to spread over a broader range (i.e.,
208 long foot at the right bottom corner in Figure 3(c)) whereas this type of long foot was not observed in
209 the central area. In the two-individual group, similarly, distribution patterns were different in the
210 boundary and the central areas, as well as “before” and “after” treatment (Figures 3(i) and (l)). A

211 detailed description of the distribution patterns, however, is beyond the scope of this study and will be
212 reported elsewhere.

213 Intermittency was further contrasted before and after treatment in Figure 4, and the probability
214 distributions of the shadowing time were fitted to lines and exponential curves because intermittency
215 exhibited a universal algebraic scaling at high frequencies and an exponential scaling at lower
216 frequencies [28, 30]. Table 1 summarizes the slopes of the lines based on regression analyses, and
217 Table 2 lists the coefficients and fittings to the exponential functions in the boundary and the central
218 areas for one- and two-individual groups. For the one-individual group, the probability distributions
219 were fitted to single lines (Figures 4(a) and (b), (d) and (e)). The slopes were similar and were in the
220 range of -1.89 – -1.91 for the x - component and -1.75 – -1.76 for the y -components before and after
221 treatment, but the difference in the slopes of the regression lines were not statistically significant
222 ($p>0.05$; Figures 4(a) and (b)) [56]. In the central area, however, the slopes were different for the x -and
223 the y -components of the forces. The slopes were statistically steeper for both components of the forces
224 after treatment (-1.79 – -1.80) than “before” treatment (-1.13 – -1.32) ($p<0.05$; Figures 4(d) and (e)),
225 indicating that the phase change in the shadowing time was more sensitive in the central area under
226 chemical stress.

227 For the absolute forces, the probability distributions of the shadowing time for one individual (Figures
228 4(c) and 4(f)) were more spread compared to those for the x -and the y -components of the forces in the
229 boundary and the central areas. The slopes appeared to be different, with statistical significance, before
230 and after treatment (Table 1). At the boundary area, slopes were steeper after treatment (-1.38) than
231 before treatment (-1.02) whereas slopes were less steep in the central area after treatment (-1.34) than
232 before treatment (-1.66) (Table 1).

233 Forces on the center of mass for the two-individual group were also calculated (Figures 4(g) – (l)).
234 Compared with the forces on the one-individual group (Figures 4(a) – (f)), the probability distributions

235 of the shadowing time were different, showing two phases as stated above. In both the x - and the y -
236 components, intermittency appeared to be curved with a breakpoint in the boundary (Figures 4(g) – (h))
237 and the central (Figures 4(j) – (k)) areas whereas single lines were fitted to the intermittency curves for
238 the case of the one-individual group (Figures 4(a), (b) and (d), (e)), as stated above. The breakpoint was
239 found to be around 10 seconds, and intermittency was overall similar between the boundary and the
240 central areas for the two-individual group. It was remarkable that the difference in intermittency before
241 and after treatment was more clearly observed in the boundary area (Figures 4(g) and (h)), contrary to
242 the case of the one-individual group where the difference was only observed in the central area (Figures
243 4(d) and (e)) (Table 1). It is also noteworthy that after treatment, the elevation of the intermittency (i.e.,
244 intercepts of regression lines) was lower in both the x - and the y -components in the boundary area
245 (Figures 4(g) and (h)). A statistical difference between the boundary and the central areas was observed
246 for the absolute forces (Figures 4(i) and (l), Table 1).

247 For the absolute forces on two individuals, curves were also formed in the boundary area, more
248 strongly for “after” treatment (Figure 4(i)) although higher variation was observed in probabilities
249 compared to the x and the y -components of the forces (Figures 4(g) and (h)). The breakpoint appeared
250 to slightly move toward long time duration, a little over 10 seconds (Figure 4(i)). The lines fitted to the
251 probability distributions at high frequency (i.e., before breakpoint) were statistically different before (-
252 0.89) and after (-1.19) treatment in the boundary area (Table 1). In the central area, however, single
253 lines were fitted to probability distributions across the shadowing time, and the slopes (-0.94 and -0.96)
254 were not statistically different (Table 1). We also fitted the intermittency at lower frequency (i.e., a
255 long shadowing time after breakpoint) to an exponential function [28, 30]. The coefficients were in the
256 range of 0.30 – 0.34 and exponential curves before and after treatment were not statistically different
257 when the goodness of fit between the two curves was tested according to the chi-square test [56] (Table
258 2). Although not presented in the figures, intermittency curves for velocities observed at the boundary

259 and the central areas were similar to the case of forces (center of mass) both “before” and “after”
260 treatment. However, the intermittency of velocities was weaker in expressing the difference between
261 “before” and “after” treatment.

262 We also calculated the relative forces between two individuals in the two-individual group (Figures
263 5(a) – (f)). Similar to force of center of mass (Figures 4(g) – (l)), two phases were observed around the
264 breakpoint of 10 seconds. The shapes of the probability distributions before and after treatment were
265 different in the boundary area while the shapes were similar in the central area. Statistical significance
266 was observed in the lines fitted to the intermittency in the x - and the y -components for the short-time
267 duration before and after treatment (Table 1) (Figures 5(a) and (b)). The slopes ranged from -0.90 to -
268 1.10 before treatment and from -1.09 to -1.63 after treatment for the x - and the y -components in the
269 boundary and the central areas. The slopes were statistically different before and after treatment in the
270 boundary area (Table 1). Although the slopes were not different in the central area, the elevations (i.e.,
271 y -intercepts of the regression lines) were statistically different before and after treatment (see Ref. 56
272 for the statistical significance of the elevation in a regression line).

273 For absolute forces, the probability distributions were also different before and after treatment
274 (Figures 5(c) and (f)). A breakpoint was observed, and the point appeared to move more toward the
275 long-time duration, approximately matching 25 seconds in the boundary area. The slopes (-0.76 – -0.89)
276 of the regression lines for the absolute force were less steep compared to those of the x - and the y -
277 components (-0.90 – -1.63) in the boundary area and were comparable to those of the absolute forces (-
278 0.94 – -0.96) on the center of mass in the center area (Table 1). The coefficients (α) of the exponential
279 functions were also fitted to the probability distribution of the long shadowing time and ranged from
280 0.30 to 0.35. The exponential curves before and after treatment were not statistically different when
281 the goodness of fit between two the curves was tested according to the chi-square test [56].

282 We also checked the distribution pattern for forces for all individuals in the two-individual group
283 (Figures 5(g) – (l)). Similar to the case of intermittency of the relative force, overall probability
284 distributions were observed in two phases, single lines for short shadowing times and exponential
285 curves for long shadowing times (Figures 5(g) – (h) and (j) – (k)). According to this figure, the
286 probability distributions for the shadowing time tended to be slightly steeper in both the boundary and
287 the central areas after treatment. Difference in the slopes and the elevations were observed before and
288 after treatment for the x - and the y -components, as well as the absolute forces, and these differences
289 were statistically significant (Table 1). In the absolute forces, however, breakpoints were not clearly
290 observed in the central area (Figure 5(l)). Overall, the difference in intermittency appeared to be more
291 clearly observed in the boundary area (Table 1). Similar to the case of the relative force, intermittency
292 of individual forces was fitted to an exponential function with α values ranging from 0.30 to 0.35, and
293 the exponential curves before and after treatment were not statistically different, similar to two cases
294 above [56] (Table 2).

295 We also calculated the probability distributions of the shadowing time for two individuals' inter-
296 distance. The difference was outstanding in the boundary area before and after treatment; the curve
297 became rapidly steeper after the breakpoint (Figure 6(a)). Similar to the case of forces, the break point
298 was formed around 10 seconds. In the center, however, single lines were fitted both “before” and “after”
299 treatment. The slopes of the intermittency appeared to be flat, ranging from 0.22 to -0.26 in the
300 boundary area. The slope after treatment, however, became steeper (-0.80) than the slope before
301 treatment (-0.47) in the central area (Figure 6(b)). The slopes before and after treatment were
302 statistically different for both the boundary and the central areas (Table 1, Figure 6). Exponential
303 functions were fitted to the intermittency after treatment, with $\alpha = 0.26$ ($R^2=0.71$) in the boundary area,
304 according to chi-square-test goodness of fit [56] (Table 2).

305 IV. DISCUSSIONS AND CONCLUSIONS

306 It was remarkable that the data structure was fundamentally different between single and two
307 individuals. The breakpoints with two phases in intermittency were observed for short and long
308 shadowing times in the two-individual group (Figures 3(g), (h), (j) and (k)) whereas single lines were
309 presented in the one-individual group (Figures 3(a), (b), (d), and (e)). The linearity and the breakpoints
310 were consistently observed both “before” and “after” treatment (Figures 3 – 5). This indicates that
311 pairwise interaction between two individuals played a key role in determining movement data structure.
312 Recently, the importance of the nearest-neighbor relationship in group behavior was reported. Herbert-
313 Read *et al.* [54] demonstrated the importance of repulsion and response to a single nearest neighbor in
314 fish group–behavior dynamics. Pairwise interactions are important in qualitatively capturing the correct
315 spatial interactions in small groups of fish when compared with the observed data [57]. Our study
316 indirectly supports the significance of two-individual interactions in group formation.

317 In addition, the intermittency patterns were substantially different “before” and “after” chemical
318 exposure for different areas in the observation arena (Figures 4 – 6). The probability distributions of the
319 shadowing time were different before and after treatment in the center area for the one-individual group
320 whereas the difference was observed in the boundary area for the two-individual group. Regarding
321 behavioral-state changes (i.e., transition probability of different movement patterns), no qualitative
322 difference was observed between the boundary and the central areas [16]. Indeed, the overall patterns
323 of intermittency were similar in the boundary and the central areas (Figure 3). However, response to
324 chemical stress appeared differently according to the organism’s location in the arena. Especially, the
325 inter-distances between two individuals were markedly different “before” and “after” treatment (Figure
326 6). This further indicates that pairwise interactions are strongly reflected in the spatial dynamics in the
327 boundary area, suggesting emergence of new property in the movement data structure in responding to
328 neighbors nearby edge areas under stressful conditions. To the best of the authors’ knowledge, this is
329 the first report observing differences in the intermittency of forces on individuals in the boundary and

330 the central areas. Further study, however, is required in both the computational and the biological
331 aspects.

332 The existence of breakpoints in two-individual groups (Figures 3 – 5) also reflects critical time
333 duration for characterizing collective motion. Considering that the slopes for intermittency at short
334 times were near -1.5 and the slopes became steeper, the time duration of 10 seconds may be due to
335 behaviors stemming from the association of two individuals in a confined area (e.g., approach,
336 communication). The breakpoints moved toward longer time duration in the case of absolute forces
337 (Figures 5(c) and (i)). Currently, the mechanism of breakpoint formation is not known. This time
338 duration may also be due to an output from physiological networks [58]. In biological aspects,
339 physiological and/or molecular genetics networks could be investigated; how stereotypic changes in
340 behavioral patterns could originate from integrative actions of neural and endocrine systems [50].
341 However, the detailed mechanism is currently unknown and more research may be required in this
342 direction in the future.

343 Considering the difference in the intermittency patterns at different locations before and after
344 treatment, especially in the boundary area, the probability distributions of the shadowing time could be
345 utilized as a useful means of monitoring chemical stress. Intermittency in the inter-distance between
346 two individuals was remarkably different between “before (i.e., strong curves with a breakpoint)” and
347 “after (i.e., single line)” treatment in the boundary, as shown in Figure 5(a).

348 In this study, we did not use the abundance data for the minimal time duration (i.e., the first
349 probability matching to the shortest shadowing time); the points were not maximal in all cases (Figures
350 3 – 6). For instance, the point matching minimum time duration in Figure 4(a) showed abundance less
351 than the abundance shown by the second shortest shadowing time. Considering the negative value (-
352 1.5) of the intermittency [30], the abundance should be theoretically maximized at the shortest
353 shadowing time. The somewhat lower abundance at the minimum shadowing time indicates that the

354 shortest shadowing time is expressed in a reserved manner biologically, and this may stem from the
355 physiological and behavioral nature of the organisms. However, the reason is currently unknown. In
356 some cases, sufficient data to evaluate intermittency were not recorded. For instance, the intermittency
357 applied to the relative force in the central area, insufficient data points were collected in the central area
358 (Figures 5(d) and (e)). This may be due to the fact that more data points were recorded in the boundary
359 area. Considering that an acute response due to the olfactory stimulus of formaldehyde were generally
360 observed within 5 minutes as stated above, the observation time may not be extended due to weaker
361 response behaviors after 5 minutes, but the replication number may be increased. More data need to be
362 accumulated in a future study.

363 In this study, only one concentration of the chemical was tested. More research is needed at different
364 concentrations of chemicals in order to determine the fish's behavioral response to an increase in stress
365 levels. In the future, more than two individuals could be tested, and the contributions of additional
366 neighbors to group formation could be more closely investigated.

367 In conclusion, the intermittency of forces and inter-distances in one- and two-individual groups
368 effectively addressed the structural changes in collective motion. Whereas linearity was observed in the
369 probability distributions of the shadowing time for the one-individual group, two phases with
370 breakpoints were measured for two-individual group consisting linearity (the short shadowing time)
371 and exponential function (the long shadowing time). Furthermore, the effect of chemical stress was
372 demonstrated by using difference between the intermittencies in the boundary and the central areas.
373 Differences in the intermittency patterns appeared more clearly in the center for the one-individual
374 group, but the differences were more effectively presented in the boundary for the two-individual
375 group. Changes in the probability distributions of the shadowing time suggested that the pairwise
376 association between two individuals is essential in collective motion and group formation. The
377 sensitivities in the intermittencies evaluated for the one- and the two-individual groups in response to

378 toxic chemicals can be utilized as a means of behavioral monitoring to detect contaminants in the
379 environment.

380 **ACKNOWLEDGMENT**

381 This research was supported by the Basic Science Research Program through the National Research
382 Foundation of Korea (NRF) funded by the Ministry of Education, Science and Technology (2011-
383 0012960).

384 **REFERENCES**

- 385 [1] A. D. Lemly and R. J. F. Smith, *Ecotox. and Environ. Safe.* **11**, 211 (1986).
- 386 [2] H. Dutta, J. Marcelino, and C. Richmonds, *Arch. Int. Phys.* **100**, 331 (1992).
- 387 [3] T. S. Chon, N. Chung, I. S. Kwak, J. S. Kim, S. C. Koh, S. K. Lee, J. B. Leem, and E. Y. Cha, *Environ.*
388 *Monit. Assess.* **101**, 2 (2005).
- 389 [4] J. A. Macedo-Sousa, J. L. T. Pestana, A. Gerhardt, A. J. A. Nogueira, and A. M. V. M. Soares,
390 *Chemosphere* **67**, 1665 (2007).
- 391 [5] A. Gerhardt, *Biomonitoring of polluted water: reviews on actual topics* (Trans Tech Publications, Uetikon-
392 Zuerich, 1999).
- 393 [6] I. S. Kwak, T. S. Chon, H. M. Kang, N. I. Chung, J. S. Kim, S. C. Koh, S. K. Lee, and Y. S. Kim, *Environ.*
394 *Pollut.* **120**, 672 (2002).
- 395 [7] Y. S. Park, N. I. Chung, K. H. Choi, E. Y. Cha, S. K. Lee, and T. S. Chon, *Aquat. Toxicol.* **71**, 217 (2005).
- 396 [8] B. J. Lawrence and R. J. F. Smith, *J. Chem. Ecol.* **15**, 210 (1989).
- 397 [9] C. W. Ji, S. H. Lee, K. H. Choi, I. S. Kwak, S. G. Lee, E. Y. Cha, S. K. Lee, and T. S. Chon, *Int. J. Ecodyn.*
398 **2**, 28 (2007).
- 399 [10] Y. Liu, T. S. Chon, H. K. Baek, Y. H. Do, J. H. Choi, and Y. D. Chung, *Mod. Phys. Lett. B* **25**, 1135
400 (2011a).
- 401 [11] Y. Li, J. M. Lee, T. S. Chon, Y. Liu, H. Kim, M. J. Bae, and Y. S. Park, *Mod. Phys. Lett. B* **27**, 135 (2013).
- 402 [12] P. C. Tobin and O. N. Bjørnstad, *J. Ani. Ecol.* **72**, 461 (2003).
- 403 [13] S. Dray, M. Royer-Carenzi, and C. Calenge, *Ecol. Res.* **25**, 675 (2010).

- 404 [14] T. S. Chon, Y. S. Park, K. Y. Park, S. Y. Choi, K. T. Kim, and E. C. Cho, *Appl. Entomol. and Zool.* **39**, 79
405 (2004).
- 406 [15] C. K. Kim, I. S. Kwak, E. Y. Cha, and T. S. Chon, *Ecol. Model.* **195**, 62 (2006).
- 407 [16] Y. Liu, S. H. Lee, and T. S. Chon, *Ecol. Model.* **222**, 2192 (2011b).
- 408 [17] T. V. Nguyen, Y. Liu, I. H. Jung, T. S. Chon, and S. H. Lee, *Mod. Phys. Lett. B* **25**, 1144 (2011).
- 409 [18] T. Vicsek, A. Czirók, E. Ben-Jacob, I. Cohen, and O. Shochet, *Phys. Rev. Lett.* **75**, 1227 (1995).
- 410 [19] S. V. Viscido, M. Miller, and D. S. Wethey, *J. Theor. Biol.* **208**, 315 (2001).
- 411 [20] J. K. Parrish, S. V. Viscido, and D. Grünbaum, *Biol. Bull.* **202**, 296 (2002).
- 412 [21] S. H. Lee, H. K. Pak, and T. S. Chon, *J. Theor. Biol.* **240**, 250 (2006).
- 413 [22] A. S. Kane, J. D. Salierno, G. T. Gipson, T. C. A. Molteno, and C. Hunter, *Water Res.* **38**, 3993 (2004).
- 414 [23] S. Y. Ha, S. Jung, and M. Slemrod, *J. Differ. Equations* **252**, 2563 (2012).
- 415 [24] N. S. Matuda, *Bull. of the Jpn. Soc. Sci. Fisher.* **46**, 689 (1980).
- 416 [25] S. H. Lee, *J. of Asia-Pac. Entomol.* **16**, 12(2013).
- 417 [26] K. N. Tsutomu, T. Takagi, K. Yamamoto, and T. Hiraishi, *Nippon Suisan Gakkaishi* **59**, 1280 (1993).
- 418 [27] K. Suzuki, T. Takagi, and T. Hiraishi, *Fish. Res.* **60**, 4 (2003).
- 419 [28] J. E. Hirsch, B. A. Huberman, and D. J. Scalapino, *Phys. Rev. A* **25**, 519 (1982).
- 420 [29] W. C. B. David, K. Sauer, and R. J. Otis, *J. Environ. Eng. Div.* **102**, 790 (1976).
- 421 [30] Y. Do, Y. C. Lai, and Z. Liu, *E. J. Kostelich, Phys. Rev. E* **67**, 202 (2003) .
- 422 [31] Y. Do and Y. C. Lai, *Europhys. Lett.* **67**, 915 (2004).
- 423 [32] P. Manneville and Y. Pomeau, *Phys. Lett. A* **75**, 1 (1979).
- 424 [33] N. F. S. Lawrence, *Biophys. J.* **8**, 252 (1968).
- 425 [34] P. Gawthrop, I. Loram, M. Lakie, and H. Gollee, *Biol. Cybern.* **104**, 32 (2011).
- 426 [35] Y. Pomeau, J. C. Roux, A. Rossi, S. Bachelart, and C. Vidal, *J. Physique Lett.* **42**, 272 (1981).
- 427 [36] I. M. De la Fuente, L. Martinez, and J. Veguillas, *Biosystems* **39**, 88 (1996).
- 428 [37] G. J. de Valcárcel, E. Roldán, V. Espinosa, and R. Vilaseca, *Phys. Lett. A* **206**, 360 (1995).
- 429 [38] Y. Pomeau and P. Manneville, *Commun. in Math. Phys.* **74**, 190 (1980).
- 430 [39] T. Datry, D. Arscott, and S. Sabater, *Aquat. Sci.* **73**, 454 (2011).

431 [40] M. T. Bogan, K. S. Boersma, and D. A. Lytle, *Freshwater Biol.* **10**, 1111 (2013).

432 [41] A. Harnos, G. Horváth, A. B. Lawrence, and G. Vattay, *Physica A* **286**, 312 (2000).

433 [42] A. Mashanova, T. H. Oliver, and V. A. A. Jansen, *J. R. Soc. Interface* **7**, 199 (2010).

434 [43] R. Jeanson, S. Blanco, R. Fournier, J. L. Deneubourg, V. Fourcassié, and G. Theraulaz, *J. Theor. Biol.* **225**,

435 443 (2003).

436 [44] M. Martin, F. Bastardie, D. Richard, F. Burel, and C. R. Acad. Bulg. Sci. **324**, 1029 (2001).

437 [45] J. R. Fetcho and K. S. Liu, *Ann. NY Acad. Sci.* **860**, 334 (1998).

438 [46] G. R. Blaser R, *Behav. Res. Methods* **38**, 456 (2006).

439 [47] E. Levin, Z. Bencan, and D. Cerutti, *Physiol. and Behav.* **90**, 55 (2007).

440 [48] S. Kato, *J. Neurosci. Methods* **134**, 2 (2004).

441 [49] H. A. Swain, C. Sigstad, and F. M. Scalzo, *Neurotoxicol. and Teratol.* **26**, 726 (2004).

442 [50] R. Gerlai, V. Lee, and R. Blaser, *Pharmacol. Biochem. Behav.* **85**, 753 (2006).

443 [51] N. Miller and R. Gerlai, *Behav. Brain Res.* **184**, 157 (2007).

444 [52] N. Noordiana and Y. C. B. Farhana, *Int. Food Res. J.* **18**, 125 (2011).

445 [53] C. Xia, Y. Li, T. S. Chon, and J. M. Lee, *Indust. Elec. ISIE*, 909 (2009).

446 [54] J. E. Herbert-Read, A. Perna, R. P. Mann, T. M. Schaerf, D. J. T. Sumpter, and A. J. W. Ward, *P. Natl. A.*

447 *Sci.* **108**, 18726 (2011).

448 [55] R. D. Collins, R. N. Gargesh, A. D. Maltby, R. J. Roggero, M. K. Tourtellot, and W. J. Bell, *Physiol.*

449 *Entomol.* **19**, 166 (1994).

450 [56] J. H. Zar, *Biostatistical analysis* (Prentice hall, Upper Saddle River, New Jersey, 1999).

451 [57] Y. Katz, K. Tunstrøm, C. C. Ioannou, C. Huepe, and I. D. Couzin, *P. Natl. A. Sci.* **108**, 18720 (2011) .

452 [58] I. D. Couzin, J. Krause, R. James, G. D. Ruxton, and N. R. Franks, *J. Theor. Biol.* **218**, 2 (2002).

453 Table 1 Estimates of the slopes and elevations by applying a regression analysis to the intermittency
 454 of forces for movement of zebrafish in one- and two-individual groups in the boundary and central
 455 areas before and after chemical treatment.

No. of indi	Type	Treat	Boundary			Center		
			X	Y	Absolute	X	Y	Absolute
One	Indi	Before	-1.89±0.20	-1.76±0.19	-1.02±0.27	-1.32±0.16	-1.13±0.16	-1.66±0.49
		After	-1.91±0.19	-1.75±0.19	-1.38±0.26*	-1.79±0.11*	-1.80±0.18*	-1.34±0.11*
	Center of mass	Before	-1.11±0.17	-1.10±0.11	-0.89±0.11	-1.08±0.15	-1.17±0.18	-0.94±0.26
		After	-1.61±0.17*	-1.48±0.14*	-1.19±0.16*	-1.26±0.32*	-1.14±0.26*	-0.96±0.31
Two	Relative	Before	-1.09±0.13	-1.1±0.09	-0.79±0.18	-0.90±0.19	-1.07±0.15	-0.76±0.32
		After	-1.63±0.16*	-1.41±0.09*	-0.89±0.14 ^①	-1.30±0.22 ^②	-1.09±0.20 ^③	-0.87±0.40*
	Indi	Before	-1.35±0.11	-1.28±0.08	-0.71±0.15	-0.94±0.10	-1.07±0.12	-0.79±0.06
		After	-1.61±0.17*	-1.52±0.09*	-0.89±0.16*	-1.03±0.19 ^④	-1.02±0.17 ^⑤	-1.03±0.07*

456
 457 * Indicates statistical significance “before” and “after” treatment based on the different slopes of the regression lines ($p < 0.05$) [56].
 458 Numbers in circles present statistical significances “before” and “after” treatment based on the different elevations in the regression
 459 lines ($p < 0.05$) [56] ①-2.07/-1.50, ②-1.15/-0.97, ③-1.08/-0.81, ④-1.40/-1.17 and ⑤-1.47/-1.10, before /after treatment, respectively.

460

461 Table 2 Estimates of the coefficient (α) of the exponential function and the goodness of fit (chi-square test)

462 applied to the intermittency of forces of zebrafish in one- and two-individual groups before and after treatment.

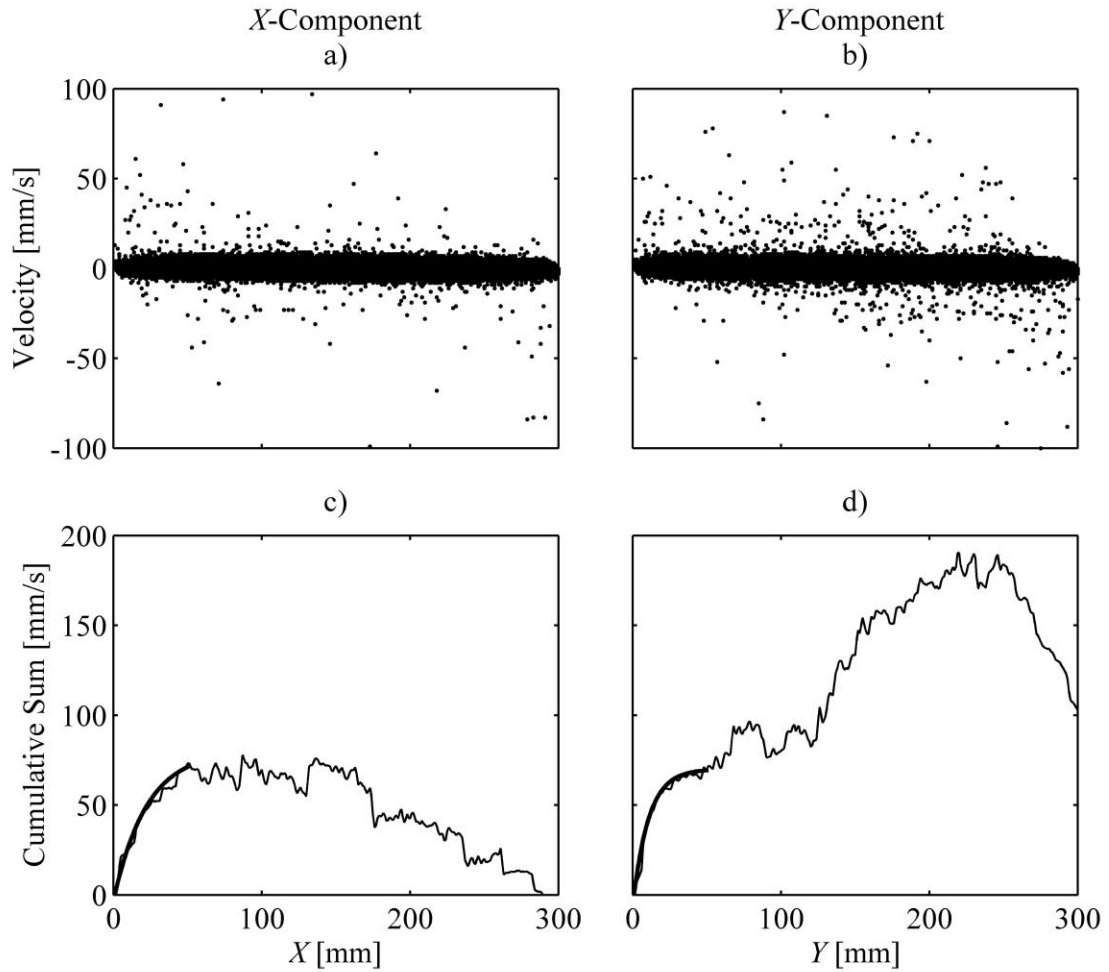
Type	Treat Test	Boundary		Center	
		X	Y	X	Y
Center of mass	Before †	0.31 (0.42)	0.30 (0.41)	0.30 (0.59)	0.30 (0.36)
	After †	0.35 (0.61)	0.34 (0.62)	0.30 (0.30)	0.30 (0.25)
	χ^2 ††	10.66 (0.15)	10.14 (0.18)	0.63 (1.00)	1.79 (0.97)
Relative	Before	0.30 (0.64)	0.31 (0.45)	0.30 (0.56)	0.31 (0.27)
	After	0.35 (0.79)	0.33 (0.85)	0.31 (0.30)	0.31 (0.56)
	χ^2	10.28 (0.17)	11.72 (0.11)	5.61 (0.59)	11.89 (0.10)
Indi	Before	0.33 (0.48)	0.33 (0.52)	0.30 (0.34)	0.30 (0.29)
	After	0.35 (0.58)	0.35 (0.52)	0.30 (0.61)	0.31 (0.41)
	χ^2	3.79 (0.80)	3.19 (0.87)	5.30 (0.63)	7.67 (0.47)

463

464 † Numbers in parentheses indicate the R^2 value according to the coefficient estimate of the functions (exponential decay [56]).

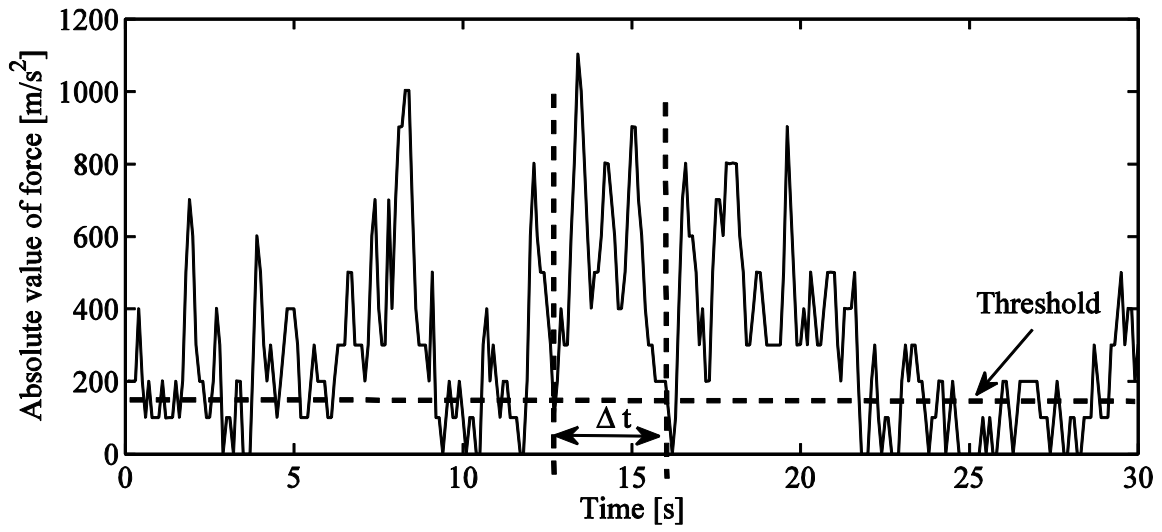
465 †† Numbers in parentheses present the probability according to chi-square test's goodness of fit between two exponential functions, one

466 before and one after treatment [56].



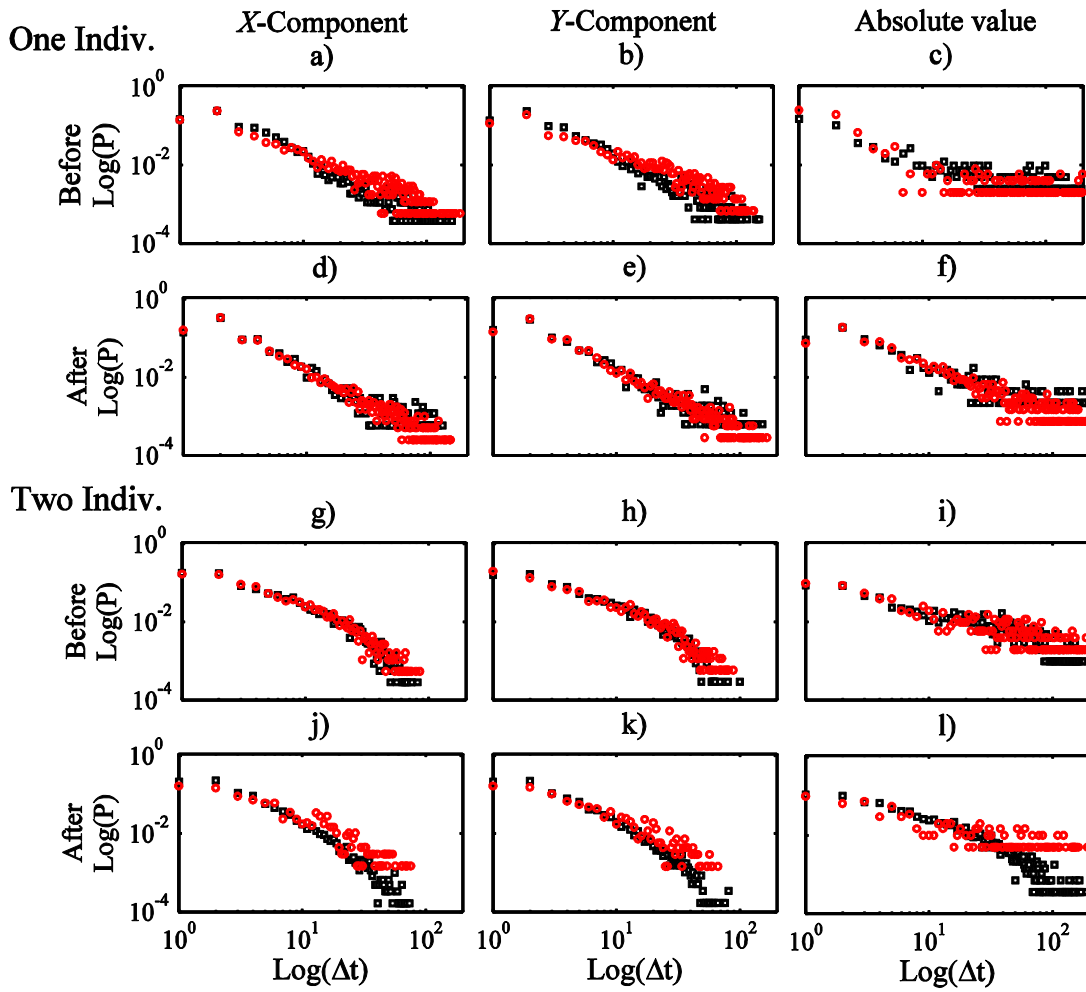
467

468 Fig. 1. Velocity distribution and its cumulative sum along each axis of fish movement in the
 469 observation arena in defining the boundary area: (a) x -component, (b) y -component, (c) cumulative
 470 sum of the x -component, and (d) cumulative sum of the y -component. Solid curves at the boundary (c)
 471 and (d) indicate the exponential curves fitting the data from 0 mm to 50 mm.



472

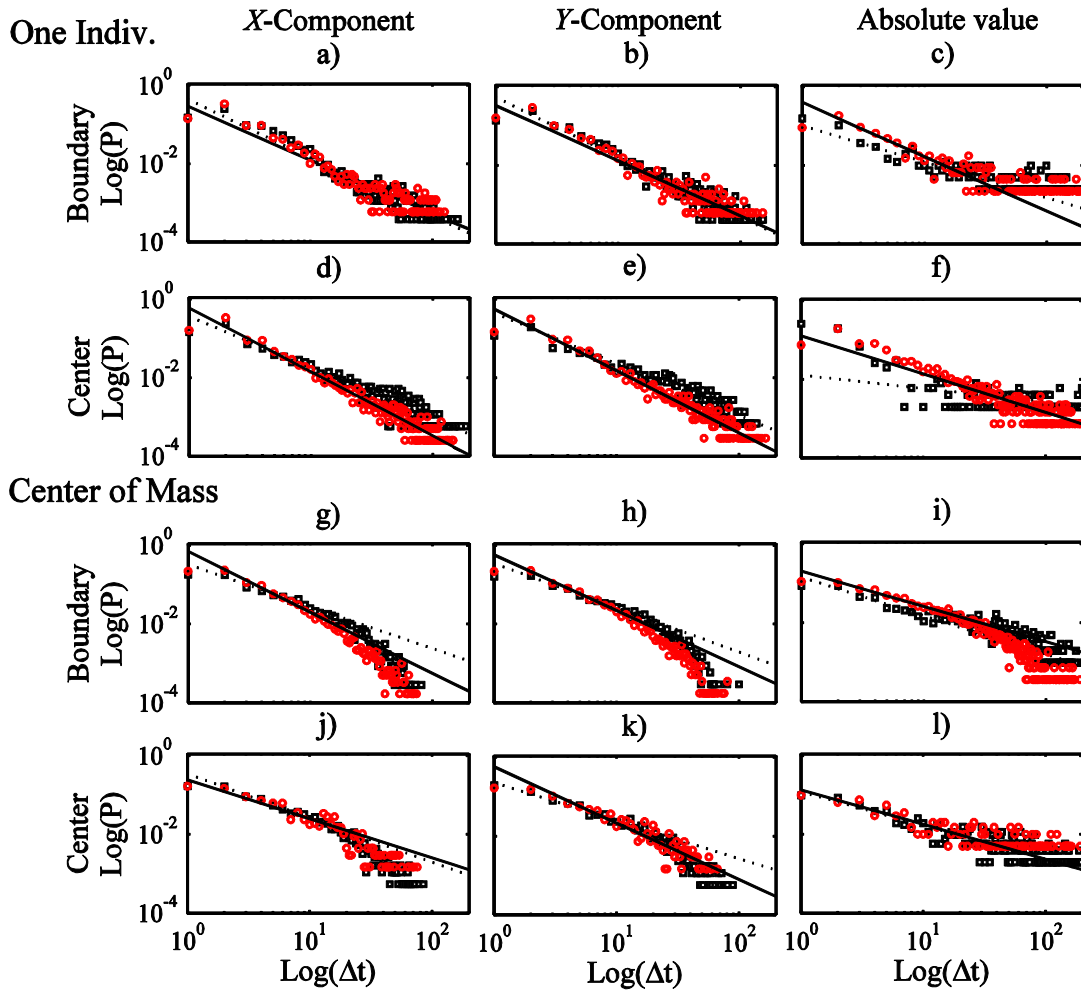
473 Fig. 2. Time series of the absolute value of force for one individual before treatment in the center for
 474 various shadowing times (Δt) and a threshold (dashed line) to determine the shadowing time.



475

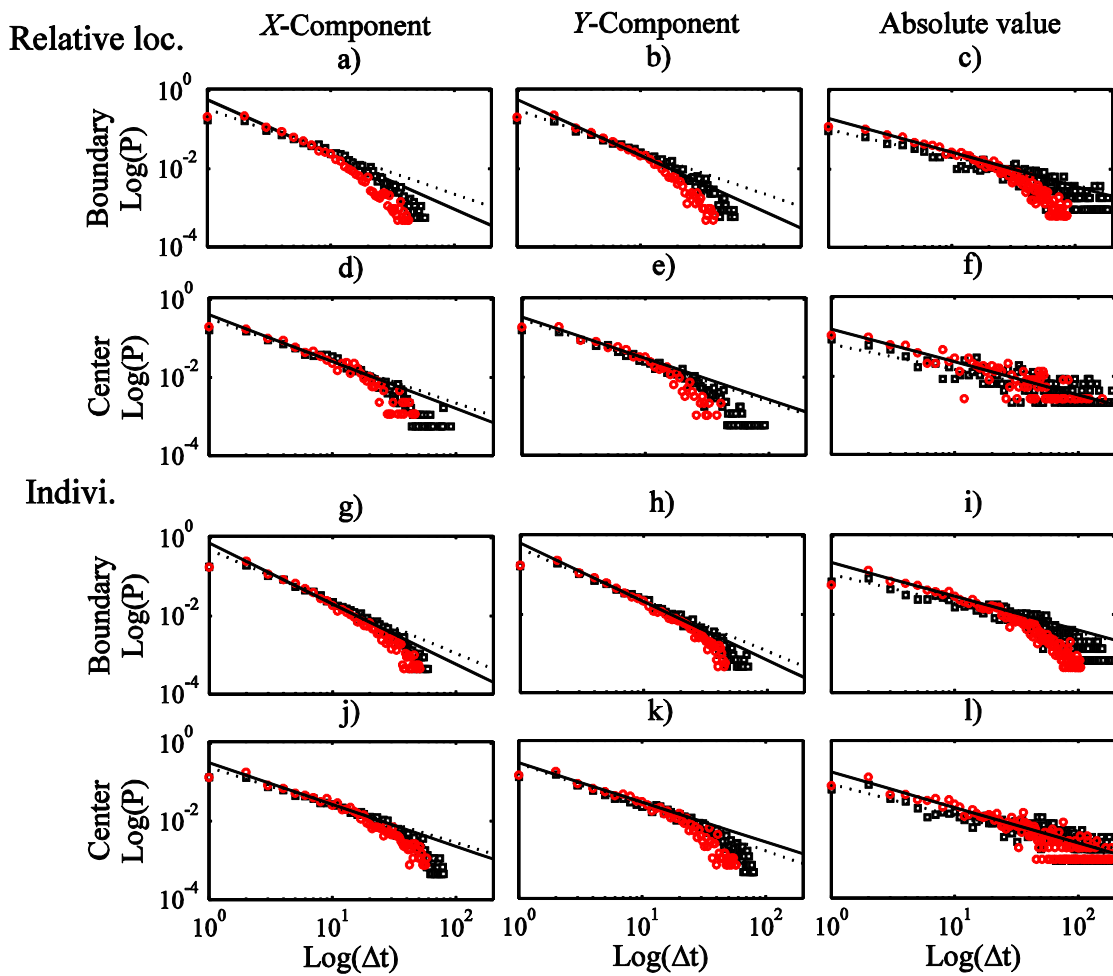
476 Fig. 3. Intermittency patterns for forces on one individual before (a, b, and c) and after (d, e, and f)
 477 treatment, and those for two individuals before (g, h, and i) and after (j, k, and l) treatment in the
 478 boundary (blank squares) and the central (red circles) areas. The probability distributions of the
 479 shadowing time were fitted to single lines for the one-individual group whereas they were matched to
 480 exponential curves for the two-individual group.

481



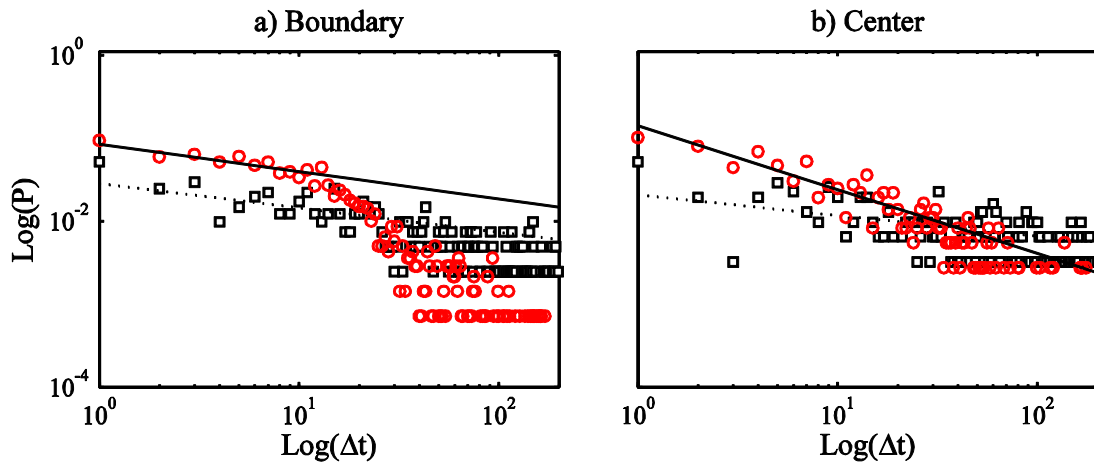
482

483 Fig. 4. Intermittency patterns for the forces on the one-individual group in the boundary area ((a) x -
 484 components, (b) y -component, and (c) absolute value) and in the central area ((d) x -component, (e) y -
 485 component, and (f) absolute value), and those for force at the center of mass of the two-individual
 486 group in the boundary area ((g) x -component, (h) y -component, and (i) absolute value) and the central
 487 area ((j) x -component, (k) y -component, and (l) absolute value). Intermittency patterns before and after
 488 treatment were different in the center for the one-individual group whereas the difference was observed
 489 in the boundary for the two-individual group. Solid and dotted lines fitting “before” and “after”
 490 treatment, respectively.



491

492 Fig. 5. Intermittency patterns for the forces before (blank squares) and after (red circles) treatment in
 493 the two- individual group. The relative force on individuals in the boundary area ((a) x -component, (b)
 494 y -component, and (c) absolute value) and in the central area ((d) x -component, (e) y -component, and (f)
 495 absolute value), and those on two individuals in the boundary area ((g) x -component, (h) y -component,
 496 and (i) absolute value) and in the central area ((j) x -component, (k) y -component, and (l) absolute
 497 value). Differences in the intermittency patterns before and after treatment were more clearly observed
 498 in the boundary for relative forces whereas the difference was equally observed in the boundary and the
 499 center for individual forces. Solid and dotted lines fitting “before” and “after” treatment, respectively.



500

501 Fig. 6. Intermittency patterns for the inter-distance between two individuals before (blank squares)
 502 and after (red circles) treatment in (a) the boundary (slopes before (-0.22 ± 0.08) and after (-0.26 ± 0.12)
 503 treatment), and (b) the center (slopes before (-0.47 ± 0.06) and after (-0.80 ± 0.11) treatment). The
 504 intermittency pattern was markedly different after treatment in the boundary with a breakpoint clearly
 505 separating flat (for short shadowing time) and steep (for long shadowing time) slopes. Solid and dotted
 506 lines fitting “before” and “after” treatment, respectively.